Flexible tuning microwave permeability spectrum in [ferromagnet/antiferromagnet]$_n$ exchange-biased multilayer stack structure*

Jin Li-Chuan(金立川)†, Zhang Huai-Wu(张怀武), Tang Xiao-Li(唐晓莉), Bai Fei-Ming(白飞明), and Zhong Zhi-Yong(钟智勇)

State Key Laboratory of Electronic Thin Films and Integrated Devices, University of Electronic Science and Technology of China, Chengdu 610054, *China*

(Received 9 July 2012; revised manuscript received 28 September 2012)

NiFe/[IrMn/NiFe/IrMn]$_5$/[NiFe/IrMn]$_4$/NiFe structured exchange-biased multilayer films are designed and prepared by magnetron sputtering. The static and the microwave magnetic properties are systematically investigated. The results reveal that adding a partially pinned ferromagnetic layer can effectively broaden the ferromagnetic resonance linewidth toward the low frequency domain. Moreover, a wideband multi-peak permeability spectrum with a 3.1-GHz linewidth is obtained by overlapping the spectra of different partially pinned ferromagnetic layers and [antiferromagnet/ferromagnet/antiferromagnet]$_n$ stacks. Our results show that the linewidth of the sample can be feasibly tuned through controlling the proper exchange bias fields of different stacks. The designed multilayered thin films have potential application for a tunable wideband high frequency noise filter.

Keywords: magnetic multilayer thin films, ferromagnetic resonance, permeability spectra, exchange bias

PACS: 75.30.Et, 75.60.Ej, 75.70.Cn **DOI:** 10.1088/1674-1056/22/4/047502

1. Introduction

With the rapid development of microwave integrated circuits, gigahertz range band mobile communication and radar system, high frequency noises of the microwave devices, and transmission lines become a potential problem for the modern information systems and may even pose a health risk to humans. Therefore, it is crucial to suppress the electromagnetic noises. A microwave noise filter based on soft magnetic thin films has been proposed and intensively investigated in recent years.[1,2] Most of the researchers made their efforts to adjust the ferromagnetic resonance (FMR) frequency (f_r) to a higher frequency domain. These include patterning magnetic films into strip structures,[3] doping the third element into the ferromagnetic alloy film[4,5] and forming multilayers.[6,7] On the other hand, the exchange bias coupling effect between ferromagnetic (FM) and anti-ferromagnetic (AF) can also be used to tune FMR frequency.[8,9] All of these efforts aim to acquire a large magnetic anisotropy field H_k. As is well known, the FMR frequency in the film plane can be expressed as $f_r = \gamma/2\pi\sqrt{H_k(H_k+4\pi M_s)}$, where γ is the gyro-magnetic ratio and M_s is the saturation magnetization of the thin films.

For wideband microwave noise filter application, however, magnetic films with a broad FMR linewidth are very important. In the present work, ferromagnetic NiFe and anti-ferromagnetic IrMn are used to construct both partially pinned NiFe layers and [IrMn/NiFe/IrMn]$_n$ multilayer film stack structure with different exchange bias fields. Through overlapping the microwave permeability spectra of the partially pinned FM layers and fully pinned [AF/FM/AF]$_n$ stacks, the whole FMR frequency linewidth of the multilayer film stack structure can be greatly broadened. Furthermore, both the resonance frequency and the linewidth of the FMR frequency can be feasibly tuned by controlling proper exchange bias field of partially pinned FM layers and [AF/FM/AF]$_n$ stacks.

2. Experimental procedure

[$Ni_{81}Fe_{19}$/$Ir_{19}Mn_{81}$]$_n$ exchange-biased multilayer stacks are prepared on Si (100) substrates by dc magnetron sputtering. The base vacuum and working pressure are 7×10^{-6} Pa and 7.2×10^{-2} Pa, respectively. The deposition rates for all the layers are all approximately 0.1 nm/s and controlled by a quartz-crystal deposition monitor. A magnetic field of about 30 mT is applied along the substrate surface during thin films growth process to induce the necessary exchange bias.[10] The static magnetic properties of the samples are measured by using a vibrating sample magnetometer (VSM). The permeability spectra in a frequency range from 0.05 GHz–6 GHz are obtained by using a shorted micro-strip transmission line perturbation method[11] with Agilent 4285 vector network analyzer.

*Project supported by the Foundation for Innovative Research Groups of the National Natural Science Foundation of China (Grant No. 61021061), the National Basic Research Program of China (Grant No. 2012CB933104), and the National Natural Science Foundation of China (Grant Nos. 61071028, 51171038, and 60801027).

†Corresponding author. E-mail: brooklynlichuanj@gmail.com

© 2013 Chinese Physical Society and IOP Publishing Ltd

3. Results and discussion

Figure 1 shows the microwave permeability spectra and magnetic hysteresis loops of [NiFe(30 nm)/IrMn(15 nm)]$_{10}$ and [NiFe(40 nm)/IrMn(15 nm)]$_{10}$ multilayer films. It can be clearly seen that the real and the imaginary permeability spectra each show a double-peak feature. For the [NiFe(30 nm)/IrMn(15 nm)]$_{10}$ multilayer film, the two FMR frequencies are 2.33 GHz and 3.21 GHz as shown in Fig. 1(a). With NiFe layer thickness increasing to 40 nm, the FMR frequencies reduce to 2.07 GHz and 2.76 GHz, respectively as shown in Fig. 1(c).

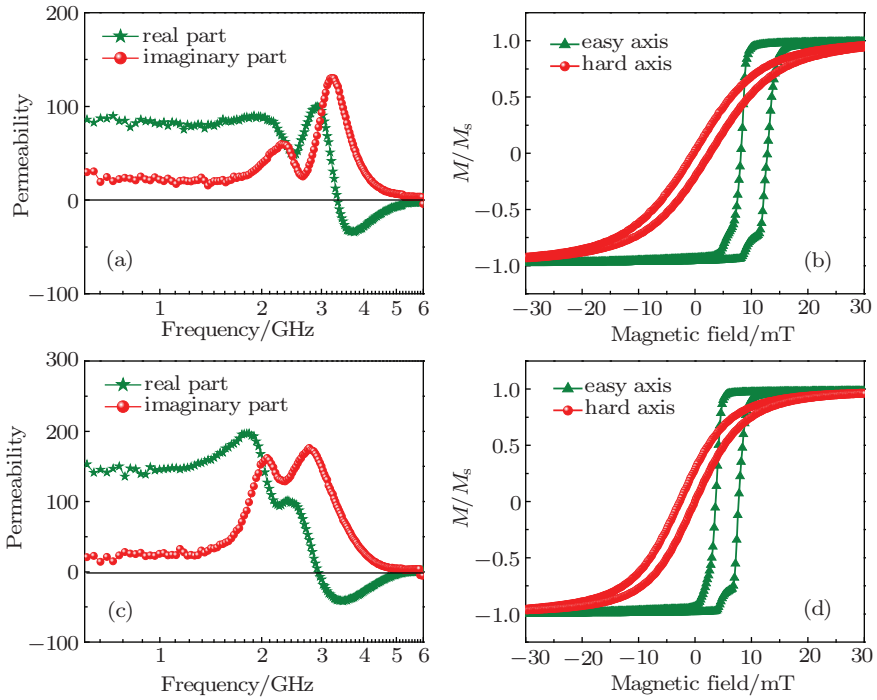


Fig. 1. (color online) (a) Permeability spectra and (b) magnetization hysteresis loops of [NiFe(30 nm)/IrMn(15 nm)]$_{10}$ exchange-biased multilayered films. (c) Permeability spectra and (d) magnetization hysteresis loops of [NiFe(40 nm)/IrMn(15 nm)]$_{10}$ exchange-biased multilayered films.

The reason for this double-peak property can be understood by the different values of exchange bias field H_{ex} acting on the various NiFe layers. The bottom NiFe layer is a partially pinned layer by its neighboring IrMn layer. However, the other nine NiFe layers are fully pinned by contacting two IrMn layers. This can be seen from the magnetization hysteresis loops as shown in Figs. 1(b) and 1(d), where a small shoulder is present in the fourth quadrant. The partially pinned NiFe layer brings an additional FMR frequency peak in lower frequency domain due to a relatively weak H_{ex}. The detail of the partially pinned NiFe layer thickness influence of microwave permeability spectrum properties can be found in our previous work.[12] The results give a chance to manipulate the permeability spectra of the exchange-biased multilayer magnetic films in the following discussion.

The arbitrarily tunable resonance linewidth is very important for the magnetic thin films used for the wideband microwave noise filter. In the present paper, according to the spectra discussed above, two kinds of exchange-biased multilayer stack configurations are designed and fabricated with several partially pinned FM layers and [AF/FM/AF]$_n$ stacks in order to realize the tunable resonance linewidth. The structure details of the configurations are listed in Table 1. Figure 2 shows the X-ray diffraction patterns of the Ta/NiFe(60 nm)/[IrMn(15 nm)/NiFe(40 nm)/IrMn(15 nm)]$_6$ / NiFe(120 nm) multilayer stack structure (configuration I) and Ta/NiFe(60 nm)/[IrMn(15 nm)/NiFe(40 nm)/IrMn(15 nm)]$_5$ / [NiFe(30 nm)/IrMn(15 nm)]$_4$/NiFe(120 nm) multilayer stack structure (configuration II). IrMn (110) and NiFe (110) peaks appear in the in-plane θ–2θ scan as shown in Fig. 2. It is

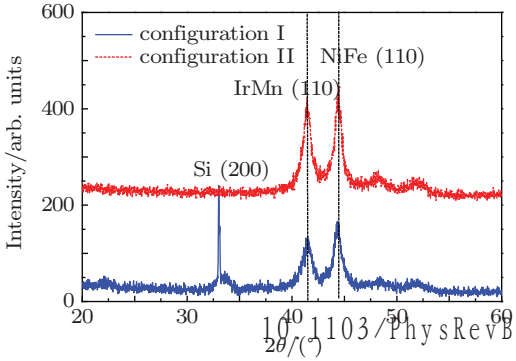


Fig. 2. (color online) XRD in-plane θ–2θ scan for configuration I and configuration II multilayer stack structures.

10.1103/PhysRevB.

noted that with the total thicknesses of IrMn and NiFe increasing, the peak intensity is enhanced and the width is narrowed, implying that the grain sizes of IrMn and NiFe increase. According to Scherrer formula and the full width at half maximum (FWHM) of the (110) peaks, for configuration I multilayer stack structure, the average IrMn grain size and NiFe grain size are estimated to be 8.9 nm and 11.5 nm, respectively. In contrast, for configuration II multilayer stack structure, the average IrMn grain size and NiFe grain size are enhanced to 10.5 nm and 13.4 nm, respectively.

Table 1. Designed and fabricated configurations with two different exchange-biased multilayer stack structures.

	Exchange-biased multilayer stacks structure
Configuration I	Ta/NiFe(60 nm)/[IrMn(15 nm)/NiFe(40 nm)/IrMn(15 nm)]$_6$/NiFe(120 nm)
Configuration II	Ta/NiFe(60 nm)/[IrMn(15 nm)/NiFe(40 nm)/IrMn(15 nm)]$_5$/[NiFe(30 nm)/IrMn(15 nm)]$_4$/NiFe(120 nm)

For configuration I, the measured magnetization hysteresis loops of the multilayer stacks along the hard and easy axes are shown in Fig. 3(a). Different exchange bias fields $H_{ex1} = 0.9$ mT, $H_{ex2} = 2.6$ mT, and $H_{ex3} = 7.1$ mT are identified from this three-stage hysteresis loop. Since the static effective anisotropy field can be obtained as $H_{keff}^{stat} = H_{ex} + H_{ua}$,[13,14] where H_{ua} is the uniaxial anisotropy field, in principle, one can easily tune the effective anisotropy field as well as the resonance frequency by changing the thickness of FM layer in both partially pinned FM layer and [AF/FM/AF]$_n$ stack structure. Therefore, tunable resonance linewidth can be realized by overlapping the adjacent resonance frequencies.

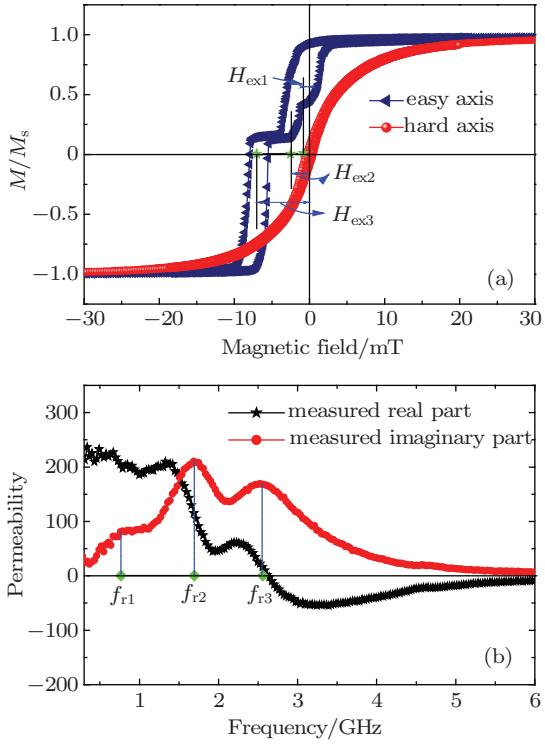


Fig. 3. (color online) (a) Magnetization hysteresis loops of configuration I. (b) Measured permeability spectra of configuration I.

Figure 3(b) shows the measured microwave permeability spectra of the Ta/NiFe(60 nm)/[IrMn(15 nm)/NiFe(40 nm) / IrMn(15 nm)]$_6$/NiFe(120 nm) multilayer stack structure. The imaginary part of the microwave permeability spectrum shows a wideband linewidth with three overlapping FMR frequencies ($f_{r1} = 0.81$ GHz, $f_{r2} = 1.69$ GHz, and $f_{r3} = 2.53$ GHz). Theoretical fitting based on the Landau–Lifshitz–Gilbert (LLG) equation is carried out to quantitatively identify the dynamic effective anisotropy field and the effective damping parameter of each FMR peak.[15–17] The fitted imaginary permeability spectrum of configuration I is shown in Fig. 4(a). Meanwhile, the dynamic effective anisotropy field (H_{keff}^{dyn}) and the effective damping parameter (α_{eff}) of each resonance frequency are shown in Fig. 4(b). Resonance frequency $f_{r1} = 0.81$ is corresponding to the top 120-nm NiFe layer, H_{keff}^{dyn} and α_{eff} are obtained to be 5.1 mT and 0.112, respectively. Due to the large anisotropy dispersion in the thick FM layer, the obtained effective damping parameter in 120-nm NiFe layer is very large. A previous report also presented the same behavior in which the FM spins near the FM/AF interface may well be aligned along the pinning direction, and the FM spins tend to be more dispersed at the center.[18] In contrast, for the bottom partially pinned 60-nm NiFe layer, its resonance frequency f_{r2} is about 1.69 GHz, and H_{keff}^{dyn} and α_{eff} are 7.2 mT and 0.056, respectively. The highest resonance frequency f_{r3} originates from the [IrMn(15 nm)/NiFe(40 nm)/IrMn(15 nm)]$_6$ exchange-biased multilayer stack, and we obtain that H_{keff}^{dyn} is equal to 12.8 mT and α_{eff} is about 0.064. It can be seen that the fitting permeability spectra are consistent with the measured multi-peak permeability spectra. Moreover, the resonance frequency linewidth is now extended from the low frequency 0.6 GHz to the very high frequency 3.2 GHz.

In order to further broaden the FMR linewidth of the magnetic films as well as to verify the above experiment results, configuration II with two partially pinned NiFe layers (bottom 60 nm, top 120 nm) and two fully pinned exchange-biased multilayer stacks ([IrMn(15 nm)/NiFe(40 nm)/IrMn(15 nm)]$_5$, [IrMn(15 nm)/NiFe(30 nm)/IrMn(15 nm)]$_4$) is designed and fabricated. Figure 5(a) shows the magnetization hysteresis loops of configuration II multilayer stack structure. From

the easy axis magnetization hysteresis loop, a clear four-stage magnetization reversal can be seen due to the overlapping of four hysteresis loops with different exchange bias fields. The exchange bias fields can be identified as $H_{ex1} = 0.5$ mT, $H_{ex2} = 2.8$ mT, $H_{ex3} = 7.3$ mT, and $H_{ex4} = 10.0$ mT. The values of uniaxial anisotropy field H_{ua} calculated from both the easy and the hard axes hysteresis loops are both 4.9 mT. Consequently, the values of static effective anisotropy field ($H_{keff}^{stat} = H_{ex} + H_{ua}$) in the exchange-biased multilayer stacks can be obtained to be $H_{keff1}^{stat} = 5.4$ mT, $H_{keff2}^{stat} = 7.7$ mT, $H_{keff3}^{stat} = 12.2$ mT, and $H_{keff4}^{stat} = 14.9$ mT, respectively.

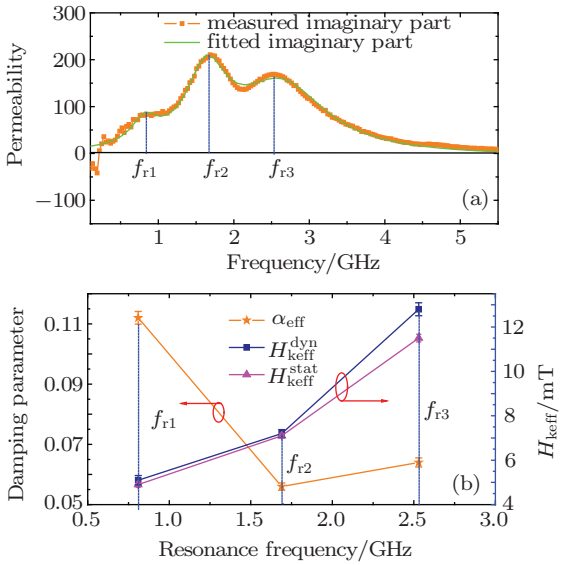


Fig. 4. (color online) (a) Curves of fitted imaginary permeability of configuration I versus frequency. (b) Effective damping parameter α_{eff}, effective dynamic anisotropy field H_{keff}^{dyn}, and effective static anisotropy field H_{keff}^{stat} versus resonance frequency.

The measured microwave permeability spectra are shown in Fig. 5(b). For the partially pinned top 120-nm and bottom 60-nm NiFe layer, its resonance frequencies f_{r1} and f_{r2} are located at 0.87 GHz and 1.83 GHz, respectively. The resonance frequencies are very close to the resonance frequency values obtained from configuration I. However, the resonance frequencies f_{r3} and f_{r4} of [IrMn(15 nm)/NiFe(40 nm)/IrMn(15 nm)]$_5$ and [IrMn(15 nm)/NiFe(30 nm)/IrMn(15 nm)]$_4$ stack are now located at 2.39 GHz and 3.24 GHz, respectively. The dynamic effective anisotropy field H_{keff}^{dyn} and the effective damping parameter α_{eff} of each resonance frequency are calculated from the theoretical fitting. As shown in Fig. 6(b), for resonance frequency $f_{r1} = 0.87$ GHz, the gained α_{eff} is 0.089, and H_{keff}^{dyn} is 4.5 mT. For resonance frequency $f_{r2} = 1.83$ GHz, α_{eff} is 0.045, and H_{keff}^{dyn} is 7.4 mT. For [IrMn(15 nm)/NiFe(40 nm)/IrMn(15 nm)]$_5$ and [IrMn(15 nm)/NiFe(30 nm)/IrMn(15 nm)]$_4$ resonance frequencies f_{r3} and f_{r4}, the values of obtained damping parameter α_{eff} and the dynamic effective anisotropy field H_{keff}^{dyn} are 0.062 and 12.8 mT, and 0.050 and 21.2 mT, respectively. As can be seen, the dynamic effective anisotropy fields are somewhat larger than the static ones obtained from the magnetization hysteresis loop. The discrepancy can be explained as the contribution of an additional rotatable anisotropy field H_{rot}, which is assumed to be related to irreversible change in AF layer and can be understood as an anisotropic field with an energetic minimum aligning parallel to FM magnetization direction.[19,20] What should be noticed is that discrepancy between H_{keff}^{dyn} and H_{keff}^{stat} increases with the thickness of the pinned NiFe layer decreasing. The discrepancy in [IrMn(15 nm)/NiFe(30 nm)/IrMn(15 nm)]$_4$ with a small NiFe thickness is up to 6.3 mT, which is much larger than the discrepancy in [IrMn(15 nm)/NiFe(40 nm)/IrMn(15 nm)]$_5$. A reasonable hypothesis to explain such a phenomenon is that the dynamic effective anisotropy of the ferromagnetic layer in FM/AF exchange bias system is composed of uniaxial anisotropy, unidirectional exchange bias, and angle-independent rotatable anisotropy,[13,21] where the rotatable anisotropy depends inversely on the FM film thickness.[21] Consequently, by overlapping the four FMR frequencies with different values of H_{keff}^{dyn}, an ultra-wide resonance linewidth imaginary permeability spectrum with a 3.1-GHz linewidth (0.6 GHz to 3.7 GHz) is experimentally achieved which is very beneficial for wideband microwave noise suppression.

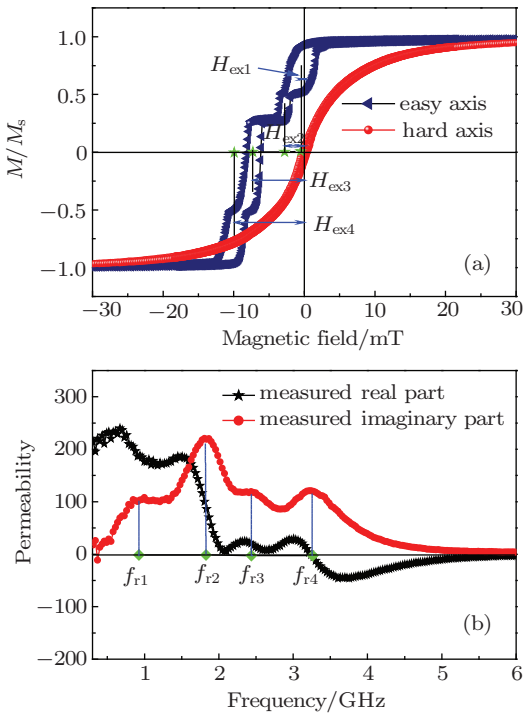


Fig. 5. (color online) (a) Magnetization hysteresis loops of configuration II. (b) Measured permeability spectra of configuration II.

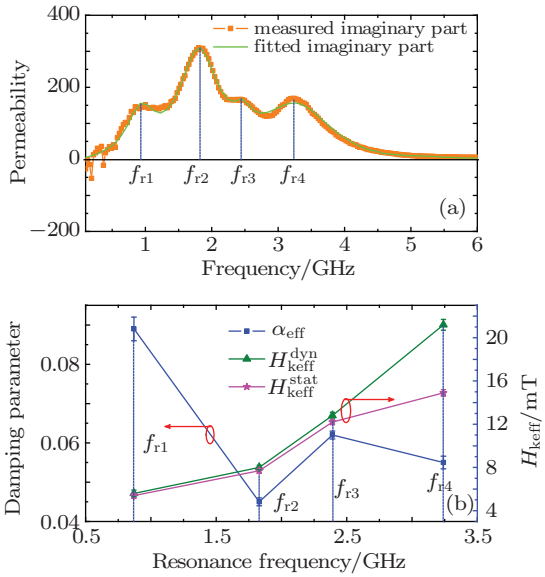


Fig. 6. (color online) (a) Curves fitted and measured imaginary permeability versus frequency of configuration II. (b) Plots of effective damping parameter α_{eff}, effective dynamic anisotropy field H_{keff}^{dyn}, and effective static anisotropy field H_{keff}^{stat} versus resonance frequency.

4. Conclusion

In this paper, we report that the microwave permeability spectrum can be flexibly tuned by a combination of partially pinned NiFe layers and $[IrMn/NiFe/IrMn]_n$ stacks with different exchange bias fields. Adding a partially pinned FM layer can effectively broaden the ferromagnetic resonance linewidth toward the low frequency domain. A wideband multi-peak imaginary permeability spectrum with a 3.1-GHz resonance linewidth is demonstrated in Ta/NiFe(60 nm)/$[$IrMn(15 nm)/NiFe(40 nm)/IrMn(15 nm)$]_5$ /$[$NiFe(30 nm)/IrMn(15 nm)$]_4$/NiFe(120 nm) configuration. Both damping parameter and effective anisotropy field of each resonance frequency are obtained by fitting the permeability spectrum based on the LLG equation. Our results provide a promising and flexible linewidth-tuning approach to microwave permeability spectra by using $[FM/AF]_n$ exchange-biased multilayer film systems. In addition, these exchange-biased multilayer thin films have a potential application to a tunable wideband high frequency noise filter.

References

[1] Phuoc N N, Xu F and Ong C K 2009 *Appl. Phys. Lett.* **94** 092505
[2] Lu G D, Zhang H W and Tang X L 2010 *Chin. Phys. Lett.* **27** 097501
[3] Chen X, Ma Y G and Ong C K 2008 *J. Appl. Phys.* **104** 013921
[4] Jiang C J, Xue D S, Guo D W and Fan X L 2009 *J. Appl. Phys.* **106** 103910
[5] Zhang L R, Lu H, Liu X, Bai J M and Wei F L 2012 *Chin. Phys. B* **21** 037502
[6] Chai G Z, Yang Y C, Zhu J Y, Lin M, Sui W B, Guo D W, Li X L and Xue D S 2010 *Appl. Phys. Lett.* **96** 012505
[7] Tang J, Ma B, Zhang Z Z and Jin Q Y 2010 *Chin. Phys. Lett.* **27** 077502
[8] Lamy Y and Viala B 2006 *IEEE Trans. Magn.* **42** 3332
[9] Phuoc N N, Lim S L, Xu F, Ma Y G and Ong C K 2008 *J. Appl. Phys.* **104** 093708
[10] Sankaranarayanan V K, Yoon S M, Kim D Y, Kim C O and Kim C G 2004 *J. Appl. Phys.* **96** 7428
[11] Liu Y, Chen L F, Tan C Y, Liu H J and Ong C K 2005 *Rev. Sci. Instrum.* **76** 063911
[12] Jin L C, Zhang H W, Tang X L and Zhong Z Y 2012 *Thin Solid Films* **520** 5756
[13] Chen J H, Tang D M, Li Y W, Zhang B S, Yang Y, Lu M and Lu H X 2010 *J. Magn. Magn. Mater.* **322** 3109
[14] Pettiford C I, Zeltser A, Yoon S D, Harri Y G, Vittoria C and Sun N X 2006 *J. Appl. Phys.* **99** 08C901
[15] Ge S, Yao S, Yamaguchi M, Yang X, Zuo H, Ishii T, Zhou D and Li F 2007 *J. Phys. D: Appl. Phys.* **40** 3660
[16] Phuoc N N, Hung L T, Xu F and Ong C K 2010 *J. Appl. Phys.* **108** 023909
[17] Yang Y, Liu L B, Tang D M, Zhang B S, Lu M and Lu H X 2010 *J. Appl. Phys.* **108** 073902
[18] Phuoc N N and Ong C K 2011 *Physica B* **406** 3514
[19] McCord J, Kaltofen R, Gemming T, Hühne R and Schultz L 2007 *Phys. Rev. B* **75** 134418
[20] Phuoc N N, Hung L T and Ong C K 2010 *J. Alloys Compd.* **506** 504
[21] Schneider M L, Kos A B and Silva T J 2005 *Appl. Phys. Lett.* **86** 202503